Ab Initio Calculations of the Vibrational and Electronic Spectra of Diketopiperazine

Jonathan D. Hirst* and B. Joakim Persson†

Department of Molecular Biology, TPC-6, The Scripps Research Institute, 10550 North Torrey Pines Road, La Jolla, California 92037

Received: June 1, 1998

One interesting feature of diamides is that, in principle, they can exhibit many of the characteristic optical properties of a helical polypeptide. Diketopiperazine (dioxopiperazine or cyclic diglycine) can perhaps be considered to be the simplest diamide, and the constraints on its conformation make it an attractive candidate for the theoretical study of the interaction between amide chromophores. We have applied correlated methods to compute *ab initio* the gas phase conformation of diketopiperazine, its vibrational spectrum, and its electronic spectrum. Using MP2 and density functional B3LYP methods, the boat conformer of the molecule and its nonsuperimposable mirror image were identified as the lowest energy structures. The planar structure was found to be a transition state. Vibrational spectra were computed for the boat and planar structures. The two boat enantiomers lie in a broad well, separated by a very small barrier corresponding to the planar form. For computational tractability, and as the barrier height is probably within the error of the calculation, we take the planar form as a representative conformation. We have computed its electronic spectrum using the complete active space (CAS) SCF method and multiconfigurational second-order perturbation theory (CASPT2). The calculated absorption spectrum is dominated by a $\pi\pi^*$ transition at 6.0 eV, with an oscillator strength in the range $f = 0.46$ to 0.58, in reasonable accord with the experimental observation of a band at 6.4 eV with an oscillator strength of $f = 0.38 \pm 0.10$. The interaction between the two amide groups is reflected in the splitting between the two $\pi\pi^*$ transitions, computed by CASPT2 to be 1.1 eV. Simply considering the interaction between the two amides as electrostatic, and treating diketopiperazine as a dimer of acetamide or a dimer of *N*-methylformamide, gives exciton splittings of 0.8 and 0.9 eV, respectively. Thus, we conclude that electrostatics dominate this interaction.

Introduction

Cyclic dipeptides, also known as diketopiperazines or 2,5-piperazinediones, are attractive model systems in which to study the interaction between two amide groups. To deepen our understanding of the optical properties of proteins, we and others have investigated the electronic structure of simple amides[1−4] using correlated *ab initio* methods. In this study, we apply such methods to compute the electronic structure of diketopiperazine (DKP), **I**. Experimental data on the electronic absorption

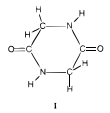

I

spectrum of DKP in gas phase,[5] solution,[5−7] and solid phase[8] are available. Ultraviolet resonance Raman studies indicate that there is significant twisting of the $\pi\pi^*$ excited state of DKP.[9] The spectra are dominated by the $\pi\pi^*$ transition which appears as a broad band, with a maximum at 7.4 eV in the gas phase, 6.4 eV in aqueous solution, and 6.6 eV in the solid phase. The gas phase data are believed to correspond to two species, the DKP monomer and the hydrogen-bonded dimer of DKP, with the gas phase maximum at 7.4 eV associated with the DKP dimer. The monomeric $\pi\pi^*$ transition was assigned to a band at 6.4 eV.[5] Our calculations are at much higher level than early semiempirical calculations,[10] which poorly described the $\pi\pi^*$ states. Thus we provide a description of the electronic structure of a diamide that is substantially more detailed and accurate than was previously available from either experimental or theoretical work.

The interactions between the two amide chromophores in cyclic dipeptides produce conformation dependent effects on the circular dichroism spectra. For this reason and because of the relative simplicity and rigidity of the structures, the circular dichroism spectra of cyclic dipeptides have been studied theoretically[11−16] and experimentally.[17−19] While many cyclic dipeptides are optically active, unsubstituted DKP itself is not, although this does not exclude the existence of equally populated, nonplanar enantiomers. The symmetry of DKP, which precludes its optical activity, is in fact an advantage when it comes to theoretical investigation as it reduces the complexity of the calculations. Despite its optical inactivity, the interaction between amides may be studied in DKP through its electronic structure. The nature of this interaction, the relative contributions of electrostatic and non-classical effects, is of particular interest. The peptide bonds in DKP are cis and they are trans in polypeptides and so DKP is not an exact model for amide interactions in polypeptides, nevertheless it is a useful one to study. Our results will provide an upper bound on the importance of nonclassical effects in the interaction between the amide groups. These effects are enhanced in DKP relative to polypeptides, as the amide groups are closer in DKP and both groups lie in the same plane. Thus, if electrostatics dom-

* To whom correspondence should be addressed. Tel: 619-784-9290. Fax: 619-784-8688. E-mail: jhirst@scripps.edu.

† National Supercomputer Centre, Linköping University, 581 83 Linköping, Sweden.

S1089-5639(98)02423-2 CCC: $15.00
Published on Web 09/01/1998

inate the interaction between the amide groups in DKP, then this result may be generalized to polypeptides where electrostatics would be expected to dominate even further.

One of the major goals of this study is to determine to what extent the interaction between the amide groups is dominated by electrostatics. The assumption that this interaction is purely electrostatic in proteins underlies currently used perturbation approaches[20−23] for calculating circular dichroism spectra of proteins. Circular dichroism is the differential absorption of left- and right-circularly polarized light. The intensity in an electronic circular dichroism spectrum is the analog of the oscillator strength in traditional absorption spectroscopy, but it is proportional to the product of the electric and magnetic transition dipole moments. Circular dichroism spectroscopy is useful for studying chiral compounds. Advances in time resolved circular dichroism, with its potential application to protein folding,[24] and the current intense focus on the characterization of the structures of peptides in solution[25] have led to a resurgence of interest in the circular dichroism of proteins. A means of calculating the circular dichroism of a polypeptide based on its three-dimensional structure, or an ensemble of structures, would be invaluable in interpreting the growing amount of experimental data. Methods for performing such calculations have been developed,[20−23] but the calculations are still more qualitative than quantitative,[26,27] and this motivates our examination of one of the fundamental assumptions of such calculations. An early study[10] compared INDO calculations of the optical activity of simple chiral cyclic amides to the perturbation approach. It was concluded that the INDO calculations were not particularly reliable for transitions beyond the lowest energy transition. Although more recent INDO/S calculations have suggested that reasonable agreement with experimental results is achieved for mono-amides,[28] rather than address this issue with semiempirical methods, we are able, with today's computational resources, to employ modern *ab initio* methods.

However, before we can compute the spectral properties of DKP, we require its geometry. The conformation of cyclic dipeptides has itself been the subject of considerable study. The crystal structure of DKP,[29] first solved by Corey in 1938[30] and the first compound containing a peptide bond to be studied by X-ray crystallography, indicates that the molecule is planar in the solid state. Nuclear magnetic resonance (NMR) studies of DKP[31,32] have produced solution phase data consistent with either a planar structure or rapidly exchanging, equally populated enantiomeric boat structures.

There have been several theoretical studies that have used empirical force fields to explore the conformational flexibility of the diketopiperazine ring.[33−35] For DKP, Karplus and Lifson[35] found a broad nonplanar minimum separated from a planar structure by less than 1 kcal/mol. Semiempirical CNDO/2 calculations[36] gave larger energy differences between planar and boat forms (up to 5 kcal/mol), but nevertheless it was concluded that external forces from a crystal or solution environment could be sufficient to enforce a planar structure. SCF calculations[37] suggested that the boat form of cyclodialanine was 7 kcal/mol more stable than the planar form, although only a minimal basis set was employed. Most recently, the gas phase conformational energetics have been investigated[38] using an empirical force field for several diketopiperazines in the context of understanding intrinsic factors governing the formation of molecular crystals known as hydrogen-bonded tapes.[39] The conformation of cyclic dipeptides thus remains a subject of current interest and furthermore, there do not appear to have been any *ab initio* studies on the conformational energetics of DKP within the last decade. Given the uncertainities surrounding the relative stabilities of the planar and boat structures of DKP, we have reinvestigated this question with current quantum chemistry methods.

Cyclic dipeptides represent an interesting series of molecules that provide an opportunity to study conformational flexibility and the influence of conformation on electronic absorption and circular dichroism. They also provide a convenient system for studying cis peptides. As a first step toward applying state of the art theoretical methods to these problems, we present MP2 and density functional B3LYP calculations of the gas phase geometry and vibrational spectrum of the simplest cyclic dipeptide, DKP, and complete active space SCF (CASSCF)[40] and multiconfigurational second-order perturbation theory (CASPT2)[41] calculations of its electronic spectrum.

Computational Details

In a semiempirical study of DKP,[36] Ciarkowski chose eight conformers typical of DKP ring folding. These structures included the planar structure and several boat forms with different degrees of twisting, both symmetric and asymmetric. Five of the basic ring structures have been observed in crystallographic studies of cyclic dipeptides other than DKP;[42−46] crystalline DKP itself is planar.[29] We used these eight structures as initial geometries. Each of these eight structures and also a chair form of DKP were optimized. Full geometry optimizations, using Gaussian94,[47] were performed using the gradient technique and second-order Møller−Plesset perturbation theory[48] (MP2) with the correlation consistent valence double-zeta basis set (cc-pVDZ).[49] All the structures converged to either a planar structure or to one of two isoenergetic enantiomeric boat forms. The planar and boat forms were also optimized using Becke's three-parameter hybrid DFT/HF method[50] using the Lee−Yang−Parr correlation functional (B3LYP) and the correlation consistent valence triple-zeta basis set (cc-pVTZ).[49] The vibrational spectra of the planar structure and one of the boat structures were computed by analytically evaluating second derivatives of the energy.

The planar B3LYP optimized structure was taken as the molecular geometry for the electronic structure calculations. The higher symmetry of the planar structure substantially simplifies the electronic structure calculation, and the choice seemed reasonable on the basis of the tiny difference in the energies of the planar and boat structures. A potential energy surface of the ground state of DKP as a function of one of the ring dihedral angles is a broad well (data not shown) indicating that DKP is quite flexible, populating both boat enantiomers, the planar structure and structures in between. The planar structure lies at the center of this broad well, and thus we choose it as representative of the ground state geometry. We calculate vertical excitation energies, and thus we do not consider the relaxation of the geometries of the excited states. Excited state calculations were performed using the CASSCF/CASPT2 method as implemented in the MOLCAS-3[51] program package. Multiconfigurational wave functions were determined using separate state-averaged CASSCF calculations for the states of different symmetry types. These wave functions were used to compute transition moments using the CAS State Interaction method (CASSI),[52] and were taken as the reference function for the CASPT2 calculation, where the second-order energies were computed. A level shift technique, the LS-CASPT2 approach,[53] was employed to avoid potential problems with intruder states. A value of 0.3 au was used for the level shift in all the computed states.

The CASSCF/CASPT2 calculations employed an atomic natural orbital (ANO) type basis set contracted to triple-ζ plus polarization quality for the first-row atoms (C, N, O 4s3p1d/H 2s1p),[54] supplemented with a 1s1p1d set of Rydberg-type functions. The Rydberg-type functions were contracted from eight primitives for each angular momentum type and were placed at the center of mass of the molecule (also the center of charge and symmetry), following the prescription of Roos et al.[55] This basis set, comprising 172 basis functions, should adequately describe the valence and Rydberg excited states. The 1s electrons of the heavy atoms were treated as frozen.

Planar DKP possesses C_{2h} symmetry. DKP is a 60 electron system and the electronic configuration of the ground state, $1\ ^1A_g$, is $(1a_g)^2...(12a_g)^2\ (1a_u)^2...(3a_u)^2\ (1b_u)^2...(12b_u)^2\ (1b_g)^2...(3b_g)^2$. Pure electronic transitions to higher A_g states are forbidden on symmetry grounds, as are transitions to B_g states. Separate state-averaged calculations were performed for the states of B_u symmetry and those of A_u symmetry, and a single root calculation was performed for the ground state. In all calculations, the first 11 orbitals of a_g and b_u symmetry and the $1b_g$ and $1a_u$ orbitals were treated as closed. In every calculation, the active space included the a_u and b_g bonding, nonbonding, and antibonding combinations of π orbitals. All but one active space (as noted below) also included the highest lone pair orbital on each oxygen atom. Only singlet states were computed.

In order to limit the size of the active space, the Rydberg 3d states were calculated with different active spaces from calculations including the Rydberg 3s and 3p states. This procedure appears to be well established.[3,4,56,57] For the A_u states, two calculations were performed each averaged over 10 states: one with an active space of ($2a_g$, $3b_u$, $4a_u$, $2b_g$), which included the Rydberg 3s and 3p orbitals, and the other with an active space comprising ($4a_g$, $1b_u$, $3a_u$, $5b_g$), in which the Rydberg 3s and 3p orbitals were deleted and replaced by Rydberg 3d orbitals of a_g and b_g symmetry. Three calculations were performed for the states of B_u symmetry, one averaged over 10 states with an active space of ($3a_g$, $3b_u$, $3a_u$, $3b_g$), which included the Rydberg 3s orbital, the Rydberg 3p orbitals of b_u symmetry and a σ^* orbital of a_g symmetry, a second averaged over two states with a ($4a_g$, $1b_u$, $3a_u$, $3b_g$) active space, with the Rydberg 3s and 3p orbitals of b_u symmetry deleted and the Rydberg 3d orbitals of a_g symmetry included, and a calculation averaged over 10 states with an active space of ($0a_g$, $0b_u$, $4a_u$, $5b_g$) which included the Rydberg 3p orbital of a_u symmetry and the Rydberg 3d orbitals of b_g symmetry. The location of the Rydberg basis functions at the center of symmetry proves to be particularly convenient in our calculations, as it permits us to use smaller active spaces than would otherwise be required. For each active space, a single root calculation of the $1\ ^1A_g$ state was performed, to provide the appropriate ground state for computing transition energies.

Results

The optimized geometries are given in Table 1; the energies are given in the legend to Table 1. Only one of the mirror images of the boat form is reported. The difference in energy between the boat and planar forms is very small. It is estimated to be 10 microhartrees (0.006 kcal/mol) by the MP2 calculation, and 126 microhartrees (0.079 kcal/mol) by the B3LYP calculation. A frequency analysis indicates that the boat form is at a minimum. The planar structure has one imaginary frequency and is thus a transition state. SCF calculations with the cc-pVDZ basis set found a chair conformation as a minimum energy structure, however, MP2 and B3LYP calculations do not show any such minimum. In Table 2 we present the calculated frequencies for the planar and boat forms. For completeness, we give both the MP2 and B3LYP results although they are very similar. There have been a number of experimental studies of the infrared spectrum of crystalline DKP,[58−60] but unfortunately there do not appear to be any infrared data for gas phase DKP. The more recent experimental data are given in Table 2, for comparison, although the effects of hydrogen-bonding are obviously not included in our calculations.

TABLE 1: The Optimized Geometries of DKP[a]

	boat structure		planar structure		
bond lengths (Å)	MP2 (VDZ)	B3LYP (VTZ)	MP2 (VDZ)	B3LYP (VTZ)	X-ray
r_{CN}	1.370	1.355	1.363	1.354	1.325
r_{CO}	1.225	1.216	1.226	1.217	1.239
$r_{CC\alpha}$	1.528	1.521	1.524	1.519	1.499
r_{NH}	1.018	1.009	1.018	1.009	0.86
$r_{NC\alpha}$	1.455	1.453	1.451	1.452	1.449
r_{CH_1}	1.109	1.095	1.104	1.092	0.95
r_{CH_2}	1.099	1.089	1.104	1.092	0.93
angles (deg)					
^{L}NCO	124.2	123.4	123.4	123.1	122.6
^{L}NCC$_\alpha$	113.7	116.2	116.8	117.1	118.9
^{L}OCC$_\alpha$	122.1	120.4	119.8	119.8	118.5
^{L}CNH	114.5	114.7	113.9	114.3	
^{L}CNC$_\alpha$	122.6	126.2	127.7	127.5	126.0
^{L}HNC$_\alpha$	118.5	118.4	118.4	118.2	
^{L}NC$_\alpha$H$_1$	112.5	111.7	110.9	110.7	
^{L}NC$_\alpha$H$_2$	109.7	109.9	110.9	110.7	
^{L}H$_1$C$_\alpha$H$_2$	107.4	107.0	106.9	106.9	
^{L}LNC$_\alpha$C	112.4	114.5	115.5	115.4	115.1
^{L}H$_1$C$_\alpha$C	107.7	107.0	106.1	106.4	
^{L}H$_2$C$_\alpha$C	106.8	106.4	106.1	106.4	
dihedrals (deg)					
^{L}OCNH	7.8	1.9	0.0	0.0	0.0
^{L}OCNC$_\alpha$	164.0	172.1	180.0	180.0	180.0
^{L}C$_\alpha$CNH	−172.5	−177.9	180.0	180.0	180.0
^{L}C$_\alpha$CNC$_\alpha$	−16.3	−7.7	0.0	0.0	0.0
^{L}NC$_\alpha$CN	−25.9	−14.8	0.0	0.0	0.0
^{L}NC$_\alpha$CO	153.8	165.3	180.0	180.0	180.0
^{L}H$_2$C$_\alpha$CN	−146.3	−136.4	123.3	123.1	
^{L}H$_2$C$_\alpha$CO	33.4	43.8	−56.7	−56.9	
^{L}H$_1$C$_\alpha$CN	98.6	109.5	−123.3	−123.5	
^{L}H$_1$C$_\alpha$CO	−81.7	−70.4	56.7	56.9	
^{L}H$_1$C$_\alpha$NC	−77.9	−98.5	−120.7	−120.8	
^{L}H$_1$C$_\alpha$NH	77.4	71.3	59.3	59.2	
^{L}H$_2$C$_\alpha$NC	162.6	142.9	120.7	120.8	
^{L}H$_2$C$_\alpha$NH	−42.1	−47.3	−59.3	−59.2	
^{L}CC$_\alpha$NC	43.9	23.2	0.0	0.0	0.0
^{L}CC$_\alpha$NH	−160.8	−166.9	180.0	180.0	180.0

[a] X-ray crystallographic data from Degeilh and Marsh.[29] The MP2/cc-pVDZ energies are −413.612945 hartrees and −413.612955 hartrees for the planar and boat structures, respectively. The analogous B3LYP/cc-pVTZ energies are −416.169205 hartrees and −416.169331 hartrees.

In Tables 3 and 4, we present the computed properties of the A_u and B_u states respectively. The oscillator strengths are calculated from the CASSCF transition moments and the CASPT2 transition energies. All permanent dipole moments are zero, due to the symmetry of the molecule. The valence and Rydberg states were readily distinguishable by their different spatial extents, as measured by the expectation value of the second Cartesian z^2-moment, $\langle z^2 \rangle$. For valence states, $\langle z^2 \rangle$ was 34 to 40 au; for Rydberg states, $\langle z^2 \rangle$ was in the range 50−100 au. In earlier calculations on mono-amides,[3,4] in order to achieve reasonable excitation energies for the valence states, it was necessary to recompute the valence states using active spaces in which the Rydberg orbitals had been deleted to compensate for so-called artificial mixing. We do not observe such mixing in our calculations, and a calculation of the B_u

TABLE 2: Calculated Frequencies in cm^{-1} [a]

boat				planar					
MP2 (VDZ)		B3LYP (VTZ)		MP2 (VDZ)		B3LYP (VTZ)		infrared data	
frequency	*I*	frequency	*I*	frequency	*I*	frequency	*I*	frequency	assignment (t)
73	5.8	54	11.8	104i	7.2	46i	9.1		
137	8.4	108	0.2	34i	0.0	90	4.0		
153	3.1	144	1.7	55	4.2	129	0.0		
413	20.6	408	27.6	407	27.8	407	29.2	447s	CO ib
413	2.4	440	2.6	434	0.0	445	0.0		
432	4.7	446	0.0	451	0.0	458	0.0		
517	65.1	510	59.1	497	57.1	500	52.4		
536	13.7	521	1.3	521	0.0	519	0.0		
607	22.5	600	5.3	602	0.0	599	0.0		
615	26.9	637	6.4	635	0.0	648	0.0		
661	111.9	664	131.0	651	159.4	667	146.3	837s	NH ob
793	2.8	774	0.1	782	0.0	766	0.0		
810	0.1	789	3.8	797	4.8	791	4.7		
910	2.0	909	15.4	926	28.2	918	29.5	913m	ring str, ring ib
1005	0.1	1013	15.1	998	0.0	1003	0.0		
1027	21.4	1016	0.0	1024	0.5	1022	0.0		
1084	58.2	1059	65.8	1082	75.3	1057	72.3	1075m	NC_α (str)
1152	2.3	1137	0.9	1176	0.0	1144	0.0		
1250	0.2	1253	1.1	1248	1.2	1253	1.9	1252w	CH_2 t
1250	1.3	1259	1.8	1262	0.0	1265	0.0		
1300	0.9	1308	0.3	1317	0.0	1312	0.0		
1342	91.8	1329	196.1	1352	120.3	1332	207.2	1343s	CH_2 wag
1389	6.0	1385	1.2	1404	0.0	1388	0.0		
1428	128.7	1425	125.5	1451	93.7	1434	126.8	1445m	CH_2 b
1464	69.8	1476	17.2	1486	0.0	1481	15.7	1470s	CN str
1477	0.8	1478	0.2	1487	41.1	1481	0.0		
1494	88.3	1504	52.2	1519	159.1	1508	60.0	1482sh	NH ib
1525	0.4	1531	0.1	1554	0.0	1537	0.0		
1820	665.1	1771	815.0	1816	701.1	1768	811.9	1697vs	CO str
1824	6.3	1774	4.2	1819	17.5	1770	0.0		
3046	39.3	3007	18.9	3087	0.0	3034	0.0		
3048	29.5	3008	35.7	3088	54.8	3035	47.4	2915w	NH str
3181	5.5	3091	8.6	3138	0.0	3061	0.0		
3182	2.6	3091	3.4	3138	18.4	3061	14.0	2986w	NH str
3625	78.3	3589	58.6	3623	79.5	3585	57.7		
3625	0.9	3590	0.6	3624	0.0	3586	0.0		

[a] Infrared intensities are given in km/mol. Experimental data are taken from a vibrational analysis of crystalline diketopiperazine.[60] Abbreviations in the assignments are ib = in-plane bend, ob = out-of-plane bend, b = bend, t = twist, str = stretch, sh = shoulder, w = weak, m = medium, s = strong, vs = very strong.

TABLE 3: The A_u Electronic States of DKP[a]

state	ΔE_{CASSCF} (eV)	ΔE_{CASPT2} (eV)	oscillator strength, *f*
1 A_u ($n\pi^*$)	8.27 [9.36]	5.32 [5.09]	0.001 [0.001]
2 A_u (π_{nb}3s)	9.43	6.08	0.001
3 A_u ($n\pi^*$)	13.93	6.57	0
4 A_u (π_{nb}3p)	10.80	6.82	0.001
5 A_u (π_{nb}3p)	10.25	6.91	0
6A_u (*n*3p)	10.82	7.10	0
7 A_u (*n*3d)	9.96	7.92	0.001
8 A_u (π_{nb}3d)	9.99	7.95	0
9 A_u (*n*3d)	10.14	8.02	0
10 A_u (π_{nb}3d)	10.36	8.25	0.004
11 A_u(π_{nb}3d)	10.48	8.54	0.006
12 A_u (π_{nb}3s)	12.59	8.84	0.018
13 A_u (π_b3p)	14.25	10.24	0
14 A_u (π_b3d)	12.42	10.35	0.006
15 A_u (π_b3p)	14.60	10.37	0.017
16 A_u (π_b3d)	12.75	10.57	0.003
17 A_u (π_b3d)	12.86	10.88	0.002

[a] Valence states appeared in both active space calculations, and those from the ($2a_g$, $3b_u$, $4a_u$, $2b_g$) calculation are shown in square brackets. The labels π_b and π_{nb} refer to bonding and nonbonding combinations of π orbitals, respectively.

TABLE 4: The B_u Electronic States of DKP[a]

state	ΔE_{CASSCF} (eV)	ΔE_{CASPT2} (eV)	oscillator strength, *f*
1 B_u ($\pi_{nb}\pi^*$)	11.01 [11.71]	5.98 [5.94]	0.580 [0.464]
2 B_u (*n*3s)	9.45	6.14	0.022
3 B_u ($\pi_{nb}3p_\pi$)	8.39	6.65	0.019
4 B_u ($\pi_{nb}\pi^*$)	12.97 [13.83]	7.09 [6.75]	0.076 [0.072]
5 B_u (*n*3p)	10.69	6.85	0.069
6 B_u (*n*3p)	11.15	7.19	0.013
7 B_u (π_{nb}3d)	9.73	7.90	0.050
8 B_u (π_{nb}3d)	9.92	7.95	0.075
9 B_u (*n*3d)	8.47	8.05	0.001
10 B_u (*n*3d)	8.67	8.31	0.005
11 B_u ($\pi_b\pi^*$)	14.11	8.74	0.246
12 B_u (π_b3p_π)	12.21	10.19	0.005
13 B_u (π_b3d)	12.37	10.22	0.032
14 B_u (π_b3d)	12.90	10.72	0.011

[a] Valence states calculated in the ($3a_g$, $3b_u$, $3a_u$, $3b_g$) active space are shown in square brackets.

valence states, in which all the Rydberg orbitals were deleted (data not shown), yielded very similar results to those reported in Table 4. The balance of the CASPT2 calculations with respect to the treatment of electron correlation may be assessed by examination of the weight ω of the CASSCF reference in the first-order wave function. For a balanced calculation, ω is similar for the ground and excited states. For the ground state and the states presented in Tables 3 and 4, the value of ω ranged from 0.70−0.78, indicating that the calculations are reasonably well balanced.

The calculated electronic spectrum is dominated by the $\pi\pi^*$ transition at 6.0 eV, with an oscillator strength of 0.58. We take the results for the B_u valence states using the active space ($0a_g$, $0b_u$, $4a_u$, $5b_g$) to be preferred, as there are a larger number of correlating π orbitals in the active space. A second, much weaker $\pi\pi^*$ transition is seen at 7.1 eV. These two transitions originate from the nonbonding π orbital. At 8.7 eV, we see a transition from the bonding π orbital to the antibonding π orbital. Its calculated oscillator strength is 0.25. Rydberg states of B_u symmetry have oscillator strengths that are an order of magnitude smaller than those of the valence states, and the oscillator strengths of the A_u states are an order of magnitude smaller again. Neither are expected to be observable in the experimental spectrum.

Discussion

There is little variation in the bond lengths (on the order of 0.01 Å) and bond angles (on the order of 1°−2°) between the planar and the boat forms, or between the MP2 and B3LYP calculations. There are substantial differences in the dihedral angles, obviously between the planar and boat forms, but also between the MP2 and B3LYP calculations. In the planar structure, the two methods give dihedral angles within 1° of each other, but in the boat form there are several dihedral angles that differ by 10°. The flexibility of the DKP molecule highlights fairly subtle differences between the results of MP2 and B3LYP, which arise from the difference in the methodologies.

The frequencies and infrared intensities computed by the MP2 and B3LYP methods are in excellent agreement. The Pearson r^2 correlation coefficient between the MP2 and B3LYP frequencies for the boat form is 0.99. The planar structure is technically a transition state (although this may be below the accuracy of the calculations), but nevertheless the planar and boat forms are expected to give similar infrared spectra. A systematic difference of $\sim$15 cm^{-1} between the carbonyl stretching bands of cyclic dipeptides in the planar and the boat conformations was recently reported based on condensed phase infrared spectroscopy.[38] In the gas phase, our calculations suggest that this difference is only 3-4 cm^{-1}. The greatest difference (and the only one larger than 10 cm^{-1}) we observe is in the NH stretch region. For the boat we see two weak peaks at 3008 and 3091 cm^{-1} which are closer together for the planar conformation, occurring at 3035 and 3061 cm^{-1}. Many of the weak transitions seen in the boat structure are not seen in the planar structure because the additional symmetry means that these transitions do not lead to any change in the dipole moment and are thus forbidden by the usual selection rules. Most of the features of the experimentally determined infrared spectrum of crystalline DKP are seen in the computed spectra. Some of the frequencies are substantially shifted, presumably due to hydrogen-bonding in the crystal structure.

The two major transitions of the calculated electronic absorption spectrum are $\pi\pi^*$ transitions at 6.0 eV (oscillator strength, $f = 0.58$) and 8.7 eV ($f = 0.25$), in reasonable agreement with the experimental observation of a band at 6.4 eV with $f = 0.38 \pm 0.10$. The lower energy $\pi\pi^*$ transition involves excitation from a nonbonding combination of π orbitals; in other amides this transition has been labeled NV_1.[61] The higher energy $\pi\pi^*$ transition involves excitation from a bonding combination of π orbitals, corresponding to the NV_2 transition in amides. We do not observe any charge transfer transitions. In a recent paper on excited state calculations of glycine and *N*-acetylglycine,[4] Serrano-Andrés and Fülscher briefly mention preliminary CASSCF/CASPT2 calculations on the linear dipeptide $CH_3-(CONH)-CH_2-(CONH)-CH_3$. The geometry was restricted to be planar and they employed basis sets of double-ζ quality. They observed NV_1 and NV_2 transitions, and also charge transfer transitions. The electronic structures of the linear dipeptide and DKP are similar. In the linear dipeptide there are two $\pi\pi^*$ NV_1-type transitions, one located on each amide group, and two $\pi\pi^*$ charge transfer transitions, involving the occupied π orbital of one amide group and the antibonding π^* orbital of the other amide group. The comparable orbitals in planar DKP, because of its high symmetry and the closer proximity of the two amide groups, are much more delocalized. However, we can still say that the two $\pi\pi^*$ states of B_u symmetry that we have reported are analogous to the localized $\pi\pi^*$ NV_1-type transition in the linear dipeptide. The $\pi\pi^*$ states of A_g symmetry, which are completely forbidden by symmetry, correspond with the two charge transfer $\pi\pi^*$ states in the linear dipeptide. These states would also be forbidden for the boat form, which has C_2, symmetry.

DKP may be considered to be a bonded dimer composed of either two acetamide molecules or two *N*-methylformamide molecules. By analyzing its electronic spectrum, we may test the approximation that the interaction between the two amide groups is solely electrostatic. It is straightforward to derive the splitting of the two monomer transitions in the dimer, and their expected intensities.[62] This splitting is known as the exciton splitting, named after a similar optical phenomenon first observed in crystals where a collective excitation takes place. For two monomer transitions in the plane, as is the case for DKP, the monomer transitions are predicted to split into a low energy transition of twice the intensity of the monomer band and a high energy transition of zero intensity. The magnitude of the splitting is given by $\Delta E = 4D/R^3$, where D is the transition dipole moment of the monomer and R is the distance between the two chromophores. We take this distance to be 2.942 Å (5.560 au), the distance between the two amide carbon atoms.

A cursory examination of the data in Table 4 indicates that our calculations qualitatively match the exciton picture, with an intense low energy $\pi\pi^*$ band and a very weak higher energy $\pi\pi^*$ band. Using the results of previous CASPT2 calculations of acetamide and *N*-methylformamide,[3] which should be comparable to our calculations of DKP, we can estimate more quantitatively how well the interaction between the two amide chromophores is approximated by the electrostatic dipole−dipole interaction. For acetamide, the CASPT2 $\pi\pi^*$ transition energy is calculated to be 7.21 eV and the oscillator strength to be 0.29, which gives a transition dipole moment of 3.26 D (1.28 au). Thus, treating DKP as a bonded dimer of two acetamide monomers gives an exciton splitting of 0.81 eV. For *N*-methylformamide, the CASPT2 $\pi\pi^*$ transition energy is 6.70 eV and its oscillator strength is 0.32, giving a transition dipole moment of 3.55 D (1.40 au). Considering DKP as a dimer of *N*-methylformamide gives an exciton splitting of 0.89 eV.

It appears that DKP may be better considered as a dimer of *N*-methylformamide than a dimer of acetamide, as the $\pi\pi^*$ transition of monomeric *N*-methylformamide lies more in the middle of the split $\pi\pi^*$ transitions of DKP. The calculated exciton splitting of 0.9 eV accounts for the majority of the *ab initio* splitting. Crudely estimating the error in the CASPT2 transition dipole moments to be $\sim$10% and given the approximation involved in describing DKP as a dimer of acetamide or *N*-methylformamide, it seems reasonable to conclude that the interaction between the two amide chromophores in DKP is well approximated by simple electrostatics.

Conclusions

Our study of DKP has applied state of the art methods to investigate a simple diamide. Although constrained, DKP is still a flexible molecule and correlated methods appear to be required to model accurately its conformational flexibility. Recent studies of mono-amides[1−4] have shown that multiconfigurational methods are needed for the theoretical study of the electronic structure of amides. We have employed such methods here to investigate a system with two interacting amide chromophores. This study is a first step towards investigating *ab initio* the role of these interactions in the optical activity of more complicated diamides. The planarity of DKP proved advantageous computationally, but it has precluded us from studying the interactions between nπ* and $\pi\pi$* states, which are also important in the optical activity of diamides and polypeptides. Nevertheless, we have gained some insight into a key interaction, that between $\pi\pi$* transitions, and the calculations presented provide a foundation on which to base further investigations of chiral diamides using similar methods.

Acknowledgment. J.D.H. thanks the National Science Foundation for financial support (Grant MCB-9632124). B.J.P. was supported by the National Science Foundation through Grant CHE-9320718 to Professor Peter R. Taylor. We thank Professor Björn Roos, Professor Peter R. Taylor and Professor Charles L. Brooks, III, for useful discussions. Computer time from the San Diego Supercomputing Center is gratefully acknowledged.

References and Notes

(1) Hirst, J. D.; Hirst, D. M.; Brooks, C. L. *J. Phys. Chem.* **1996**, *100*, 13487−13491.
(2) Hirst, J. D.; Hirst, D. M.; Brooks, C. L. *J. Phys. Chem. A* **1997**, *101*, 4821−4827.
(3) Serrano-Andrés, L.; Fülscher, M. P. *J. Am. Chem. Soc.* **1996**, *118*, 12190−12199.
(4) Serrano-Andrés, L.; Fülscher, M. P. *J. Am. Chem. Soc.* **1996**, *118*, 12200−12206.
(5) Kaya, K.; Nagakura, S. *Theor. Chim. Acta* **1967**, *7*, 124−132.
(6) Ham, J. S.; Platt, J. R. *J. Chem. Phys.* **1952**, *20*, 335−336.
(7) Nielsen, E. B.; Schellman, J. A. *J. Phys. Chem.* **1967**, *71*, 2297−2304.
(8) Kaya, K.; Nagakuru, S. *J. Mol. Spectrosc.* **1972**, *44*, 279−285.
(9) Song, S.; Asher, S. A.; Krimm, S.; Shaw, K. D. *J. Am. Chem. Soc.* **1991**, *113*, 1155−1163.
(10) Richardson, F. S.; Strickland, R.; Shillady, D. D. *J. Phys. Chem.* **1973**, *77*, 248−255.
(11) Fleischhauer, J.; Grötzinger, J.; Kramer, B.; Krüger, P.; Wollmer, A.; Woody, R. W.; Zobel, E. *Biophys. Chem.* **1994**, *49*, 141−152.
(12) Hooker, T. M.; Bayley, P. M.; Radding, W.; Schellman, J. A. *Biopolymers* **1974**, *13*, 549−566.
(13) Richardson, F. S.; Pitts, W. *Biopolymers* **1974**, *13*, 703−724.
(14) Sathyanarayana, B. K.; Applequist, J. *Int. J. Peptide Res.* **1985**, *26*, 518−527.
(15) Snow, J. W.; Hooker, T. M. *J. Am. Chem. Soc.* **1975**, *97*, 3506−3511.
(16) Snow, J. W.; Hooker, T. M.; Schellman, J. A. *Biopolymers* **1977**, *16*, 121−142.
(17) Bowman, R. L.; Kellerman, M.; Johnson, W. C. *Biopolymers* **1983**, *22*, 1045−1070.
(18) Madison, V.; Young, P. E.; Blout, E. R. *J. Am. Chem. Soc.* **1976**, *98*, 5358−5364.
(19) Strickland, E. H.; Wilchek, M.; Horwitz, J.; Billups, C. *J. Biol. Chem.* **1970**, *245*, 4168−4177.
(20) Tinoco, I. *Adv. Chem. Phys.* **1962**, *4*, 113−160.
(21) Bayley, P. M.; Nielsen, E. B.; Schellman, J. A. *J. Phys. Chem.* **1969**, *73*, 228−243.
(22) Woody, R. W. *J. Chem. Phys.* **1968**, *49*, 4797−4806.
(23) Manning, M. C.; Woody, R. W. *Biopolymers* **1991**, *31*, 569−586.
(24) Zhang, C.-F.; Lewis, J. W.; Cerpa, R.; Kuntz, I. D.; Kliger, D. S. *J. Phys. Chem.* **1993**, *97*, 5499−5505.
(25) Scholtz, J. M.; Baldwin, R. L. *Annu. Rev. Biophys. Biomol. Struct.* **1992**, *21*, 95−118.
(26) Hirst, J. D. *Enantiomer* 1998. In press.
(27) Hirst, J. D. *J. Chem. Phys.* **1998**, *109*, 782−788.
(28) Clark, L. B. *J. Am. Chem. Soc.* **1995**, *117*, 7974−7986.
(29) Degeilh, R.; Marsh, R. E. *Acta Crystallogr.* **1959**, *12*, 1007−1014.
(30) Corey, R. B. *J. Am. Chem. Soc.* **1938**, *60*, 1598−1604.
(31) Kopple, K. D.; Ohnishi, M. *J. Am. Chem. Soc.* **1969**, *91*, 962−967.
(32) Davies, D. B.; Khaled, M. A. *J. Chem. Soc. Perkin II* **1976**, 1238−1244.
(33) Ajò, D.; Granozzi, G.; di Bello, C. *Biopolymers* **1977**, *16*, 707−714.
(34) Chandrasekaran, R.; Lakshminarayana, A. V.; Mohanakrishnan, P.; Ramanchandran, G. N. *Biopolymers* **1973**, *12*, 1421−1425.
(35) Karplus, S.; Lifson, S. *Biopolymers* **1971**, *10*, 1973−1982.
(36) Ciarkowski, J. *Biopolymers* **1984**, *23*, 397−407.
(37) Støgård, Å. *Biopolymers* **1976**, *15*, 2295−2298.
(38) Palacin, S.; Chin, D. N.; Simanek, E. E.; MacDonald, J. C.; Whitesides, G. M.; McBride, M. T.; Palmore, G. T. R. *J. Am. Chem. Soc.* **1997**, *119*, 11807−11816.
(39) MacDonald, J. C.; Whitesides, G. M. *Chem. Rev.* **1994**, *94*, 2383−2420.
(40) Roos, B. O. *Adv. Chem. Phys.* **1987**, *69*, 399−446.
(41) Andersson, K.; Malmqvist, P.-Å.; Roos, B. O. *J. Chem. Phys.* **1992**, *96*, 1218−1226.
(42) Benedetti, E.; Corradini, P.; Pedone, C. *J. Phys. Chem.* **1969**, *73*, 2891−2895.
(43) Benedetti, E.; Corradini, P.; Pedone, C. *Biopolymers* **1969**, *7*, 751−764.
(44) Cotrait, M.; Ptak, M.; Bussetta, B.; Heitz, A. *J. Am. Chem. Soc.* **1976**, *98*, 1073−1076.
(45) Karle, I. L. *J. Am. Chem. Soc.* **1972**, *94*, 81−84.
(46) Lin, C. F.; Webb, L. E. *J. Am. Chem. Soc.* **1973**, *95*, 6803−6811.
(47) Frisch, M. J.; Trucks, G. W.; Schlegel, H. B.; Gill, P. M. W.; Johnson, B. G.; Robb, M. A.; Cheeseman, J. R.; Keith, T. A.; Petersson, G. A.; Montgomery, J. A.; Raghavachari, K.; Al-Laham, M. A.; Zakrzewski, V. G.; Ortiz, J. V.; Foresman, J. B.; Cioslowski, J.; Stefanov, B. B.; Nanayakkara, A.; Challacombe, M.; Peng, C. Y.; Ayala, P. Y.; Chen, W.; Wong, M. W.; Andres, J. L.; Replogle, E. S.; Gomperts, R.; Martin, R. L.; Fox, D. J.; Binkley, J. S.; Defrees, D. J.; Baker, J.; Stewart, J. P.; Head-Gordon, M.; Gonzalez, C.; Pople, J. A. *Gaussian 94* (Revision A.1); Gaussian Inc.: Pittsburgh, 1995.
(48) Møller, C.; Plesset, M. S. *Phys. Rev.* **1934**, *46*, 618−622.
(49) Dunning, T. H. *J. Chem. Phys.* **1989**, *90*, 1007−1023.
(50) Becke, A. D. *J. Chem. Phys.* **1993**, *98*, 5648−5652.
(51) Andersson, K.; Fülscher, M. P., Karlström, G.; Lindh, R.; Malmqvist, P.-Å.; Olsen, J.; Roos, B. O.; Sadlej, A. J.; Blomberg, M. R. A.; Siegbahn, P. E. M.; Kellö, V.; Noga, J.; Urban, M.; Widmark, P.-O. *MOLCAS Version 3*; Department of Theoretical Chemistry, Chemistry Center, University of Lund: Sweden, 1994.
(52) Malmqvist, P.-Å.; Roos, B. O. *Chem. Phys. Lett.* **1989**, *155*, 189−194.
(53) Roos, B.; Andersson, K. *Chem. Phys. Lett.* **1995**, *245*, 215−223.
(54) Widmark, P.-O.; Malmqvist, P.-Å.; Roos, B. O. *Theor. Chim. Acta* **1990**, *77*, 291−306.
(55) Roos, B. O.; Fülscher, M. P.; Malmqvist, P.-Å.; Merchán, M.; Serrano-Andrés, L. *Theoretical Studies of Electronic Spectra of Organic Molecules*; Roos, B. O., Fülscher, M. P., Malmqvist, P.-Å., Merchán, M., Serrano-Andrés, L., Eds.; Kluwer Academic Publishers: Dordrecht, The Netherlands, 1995; pp 357−438.
(56) Merchán, M.; Roos, B. O. *Theor. Chim. Acta* **1995**, *92*, 227−239.
(57) Serrano-Andrés, L.; Roos, B. O. *J. Am. Chem. Soc.* **1996**, *118*, 185−195.
(58) Newman, R.; Badger, R. M. *J. Chem. Phys.* **1951**, *19*, 1147−1153.
(59) Miyazawa, T. *J. Mol. Spectrosc.* **1960**, *4*, 155−167.
(60) Cheam, T. C.; Krimm, S. *Spectrochim. Acta* **1984**, *40A*, 481−501.
(61) Robin, M. B. *Higher Excited States of Polyatomic Molecules*; Academic Press, Inc.: New York, 1985; Vol. 3.
(62) Cantor, C. R.; Schimmel, P. R. *Biophysical Chemistry*; W. H. Freeman and Co.: New York, 1980; Vol. II.